JOC The Journal of Organic Chemistry

Note

pubs.acs.org/joc

Locked Planarity: A Strategy for Tailoring Ladder-Type π-Conjugated Anilido−Pyridine Boron Difluorides

Qingshan Hao,[†] Shuai Yu,[†] Shayu Li,[‡] Jinping Chen,*[,†] Yi Zeng,[†] Tianjun Yu,[†] Guoqiang Yang,*[,‡] and Yi Li*[,†]

[†]Key Laboratory of Photochemical Conversion and Optoelectronic Materials, Technical Institute of Physics and Chemistry, Chinese Academy of Sciences, Beijing 100190, China

[‡]Beijing National Laboratory for Molecular Sciences (BNLMS), Key Laboratory of Photochemistry, Institute of Chemistry, Chinese Academy of Sciences, Beijing 100190, China

Supporting Information

ABSTRACT: A novel series of *syn*- and *anti*-ladder-type anilido−pyridine boron difluorides (APBDs) were synthesized by stepwise incorporation of boron into laddered ligands. The boron coordination-locked strategy endows the ladder-type APBDs with a stiff conformation, which results in a substantial bathochromic shift of their absorption spectra and a narrowed HOMO−LUMO energy gap, reinforcing the compounds for potential applications in organic electronics.

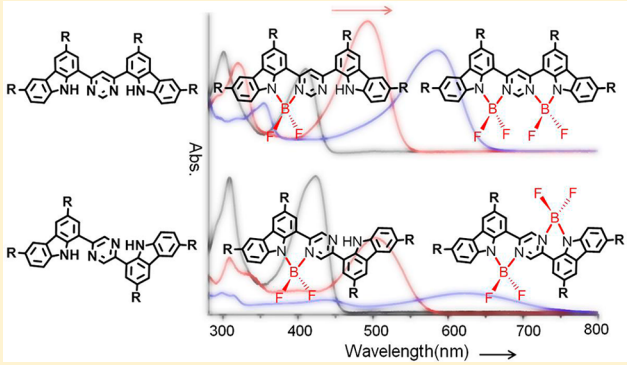

Organic conjugated molecules have drawn increasing attention because of their wide applications in electronic and optoelectronic devices, such as photovoltaic cells,[1−3] light-emitting diodes,[4−7] and field-effect transistors.[8−10] Among the classes of conjugated molecules, ladder-type π-conjugated molecules with fully ring-fused structures are particularly attractive because the flat and rigid π-conjugated skeletons endow the molecules with desired properties such as intense luminescence, good thermal stability, and high carrier mobility.[11−17] Recently, it has been demonstrated that the incorporation of boron into organic conjugated frameworks offers considerable promise for the development of new functional materials with outstanding photophysical and electronic properties.[18−24] The boron atom serves as a conduit for the π-conjugated skeleton and substantially decreases energy of the lowest unoccupied molecular orbital (LUMO), which is essential for the performance of organic electronics with high electron affinities and mobilities. Despite recent advances, examples of the incorporation boron atoms into ladder-type π-conjugated molecules are rare.[25−29]

Among boron compounds, BODIPYs have received much interest in research areas such as labeling reagents,[30−32] fluorescent switches,[33−35] chemosensors,[36−38] light-harvesting systems,[39−41] and dye-sensitized solar cells[42−44] because of their advantageous photophysical properties. The great potential has motivated the search for new π-conjugated bidentate ligands to provide boron compounds with promising electronic and optical properties.[45,46] Recently, Piers and co-wokrers reported a series of anilido−pyridine boron difluorides (APBDs), which exhibit high emission quantum yields and large Stokes shifts.[47] Inspired by their research, we anticipated that the construction of new ladder-type π-conjugated structures based on anilido−pyridine skeletons may provide molecules with the merits of both ladder-type molecules and boron compounds, which will reinforce the compounds for applications in material chemistry. Herein we report a series of *syn*- and *anti*-ladder-type APBD dyes based on the pyrimidine−carbazole and pyrazine−carbazole structures. The double-coordination endows the ladder-type APBDs with a stiff planar conformation, which allows effective π-delocalization.

The procedure for the synthesis of *syn*-ladder-type APBDs based on pyrimidine−carbazole is shown in Scheme 1. 1-Bromo-3,6-di-*tert*-butyl-9*H*-carbazole (**1**) was synthesized according to a literature procedure.[48] Borylation of **1** with pinacolborane provided 3,6-di-*tert*-butyl-1-borylcarbazole **2** in 85% yield. The Suzuki−Miyuara coupling reaction of **2** with 4,6-dichloropyrimidine afforded the *syn*-laddered ligand **3** in 70% yield. Then, treatment of **3** with excess $BF_3{\cdot}OEt_2$ furnished the corresponding *syn*-ladder-type APBD **5** in 80% yield. The ^{1}H NMR spectrum of **5** is simple, exhibiting two singlets at 9.87 and 8.62 ppm for the pyrimidine protons (H_p) along with three singlets at 8.52, 8.13, and 8.09 ppm and two doublets at 7.84 and 7.66 ppm for the carbazole protons (H_c). It shows only one characteristic peak in the ^{19}F NMR spectrum, a doublet at

Received: November 22, 2013
Published: December 4, 2013

Scheme 1. Synthesis of the Ladder-Type Ligands and APBDs

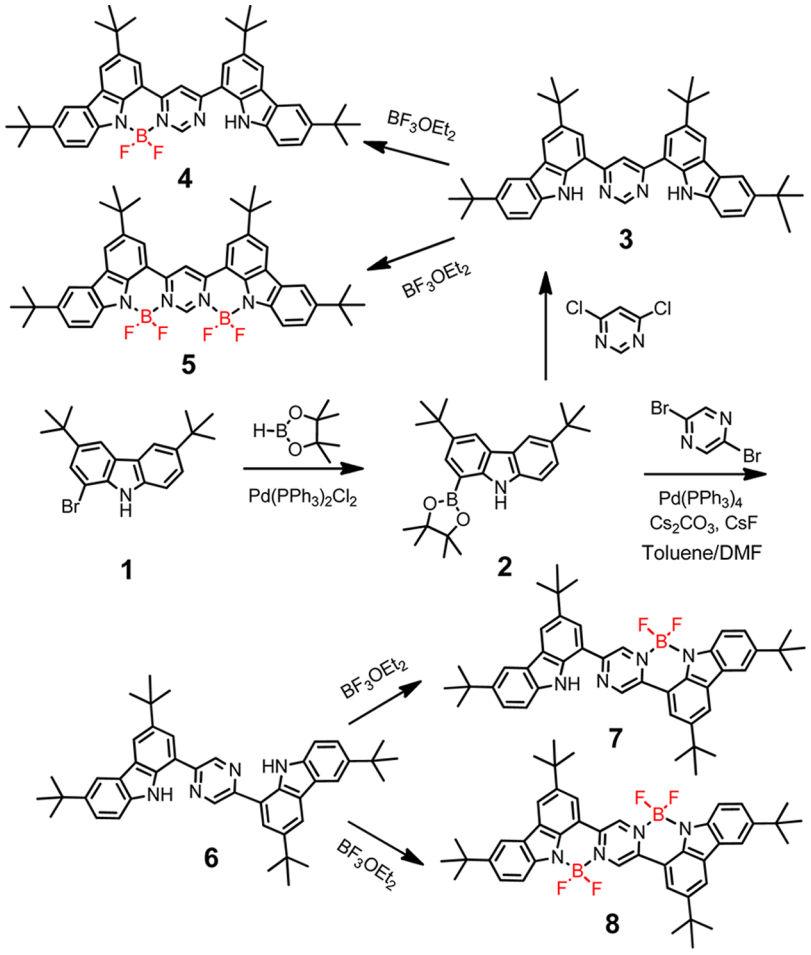

−131.6 ppm, thereby reflecting its highly symmetric structure. The parent ion peak of **5** was observed at *m*/*z* 730.5 (calcd for $C_{44}H_{48}B_2F_4N_4$ $[M]^+$: 730.4) in its MALDI-TOF mass spectrum. The high-resolution ESI-TOF mass spectrum of **5** displays only an ion peak for the ligand at *m*/*z* 657.3908 (calcd for $C_{44}H_{50}N_4Na$: 657.3933), which may be ascribed to the deborylation of **5** during the measurement. The same phenomenon was also observed for other prepared APBDs. It is worth noting that the coordination of ligand **3** with $BF_3{\cdot}OEt_2$ is a stepwise process. The monochelated ladder-type APBD **4** was obtained in 65% yield by reducing the amount of $BF_3{\cdot}OEt_2$ to 3.0 equiv and the reaction time to 1 h. The ^1H NMR spectrum of **4** exhibits an unsymmetric structure with two singlets at 10.73 and 9.57 ppm for the pyrimidine protons (H_p) and complicated signals (about 10 groups) for the carbazole protons (H_c). The ^{19}F NMR spectrum exhibits a singlet at −131.1 ppm. The parent ion peak of **4** was observed at *m*/*z* 682.5 (calcd for $C_{44}H_{49}BF_2N_4$ $[M]^+$: 682.4) in its MALDI-TOF mass spectrum.

The *anti*-ladder-type APBDs were obtained with a procedure similar to that for the *syn* ones by using 2,5-dibromopyrazine instead of 4,6-dichloropyrimidine. Treatment of **2** with 2,5-dibromopyrazine in the presence of $Pd(PPh_3)_4$ as a catalyst furnished the *anti*-laddered ligand **6** in 95% yield. The single and double chelation of **6** with $BF_3{\cdot}OEt_2$ afforded the desired *anti*-ladder-type APBDs **7** and **8** in yields of 68% and 85%, respectively, by control of the reaction conditions (Scheme 1). All of the products were fully characterized by NMR spectroscopy (^1H, ^{13}C, and ^{19}F) and mass spectrometry.

Single crystals of *syn*-laddered ligand **3** suitable for X-ray diffraction analysis were obtained by slow diffusion of methanol vapor into a toluene solution of **3**. The obtained structure is depicted in Figure 1. Obviously, the mean planes of the two carbazole rings and the pyrimidine ring take a nearly coplanar conformation, as clearly shown in the side view. The pyrimidine bridge is held to the neighboring carbazoles with a dihedral angle of 9.7°. This orientation allows **3** to coordinate with boron effectively to form the conjugated ladder-type APBDs. The crystal structure is consistent with the results from the NMR spectra, both of which indicate a symmetrical structure.

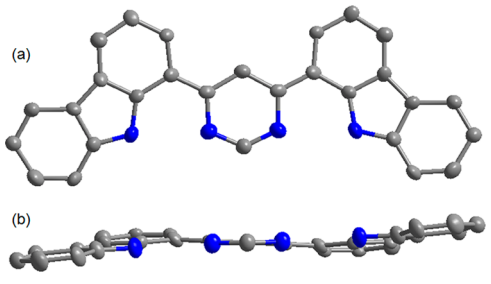

Figure 1. X-ray crystal structure of **3**: (a) top view; (b) side view. The thermal ellipsoids are shown at the 50% probability level. *tert*-Butyl groups, solvent molecules, and H atoms have been omitted for clarity.

dx.doi.org/10.1021/jo402583y | *J. Org. Chem.* 2014, 79, 459−464

The UV/vis absorption spectra of the ladder-type complexes **4**, **5**, **7**, and **8**, along with those of ligands **3** and **6**, were measured in THF and are shown in Figure 2. The *syn* ligand **3**

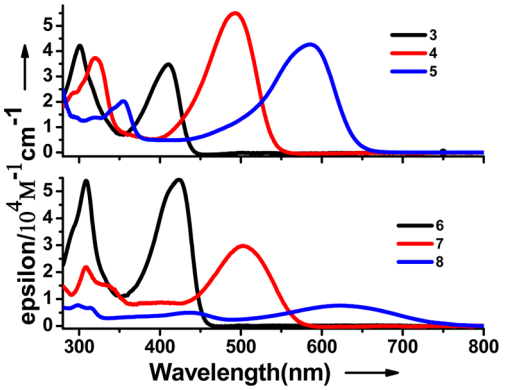

Figure 2. UV/vis absorption spectra of the *syn*- and *anti*-ladder-type APBDs and the corresponding ligands in THF.

exhibits two well-resolved absorption bands with maxima at 300 and 410 nm. The complexation of boron causes a broadening and a significant bathochromic shift of the absorption spectra. The absorption maximum shifts from 410 nm for ligand **3** to 493 and 586 nm for the mononuclear complex **4** and the dinuclear complex **5**, respectively. Apparently, the color of the solutions changes from yellow for **3** to red for **4** and dark-green for **5**, as can be observed by the naked eye. In the case of the *anti* ladders, the absorption spectra of **7** and **8** also exhibit substantial bathochromic shifts and broadening because of the complexation with boron, but the extinction coefficients decrease compared with those of the plain ligand **6**. Furthermore, the extent of the bathochromic shift is enhanced compared with the corresponding *syn* ladders, indicative of a more effective electronic delocalization through the *anti*-laddered framework. The narrowing of the HOMO−LUMO gaps (2.76, 2.25, and 1.90 eV for **3**, **4**, and **5** and 2.67, 2.13, 1.59 eV for **6**, **7**, and **8**, respectively) was estimated from the absorption spectra onsets.

No fluorescence from ligand **3** was observed with excitation at the maximal absorption wavelength of 410 nm under ambient conditions. However, the *syn*-laddered APBD **4** exhibits a broad emission band with maximum at 567 nm (Φ_f = 18%). The emission maximum of **5** shifts to 650 nm, reaching into the near-infrared spectral region with a relatively lower quantum yield (Φ_f = 6%) (see the Supporting Information). Compared with the reported carbazole−pyridine-based APBD monomer (λ_{max} = 510 nm, Φ_f = 62%),[47] the decreased emission efficiency of the *syn*-laddered **APBD** can be attributed to the enhanced conjugation, which reduces the HOMO−LUMO energy gap and consequently accelerates the nonradiative decays according to the energy gap law. In the case of the *anti*-APBD ladders (**7** and **8**), no fluorescence at longer wavelength was observed at room temperature, suggesting that the nonradiative decays dominate the photophysical processes of the excited states. A comparative study suggests more effective electronic delocalization in the *anti* framework than in the *syn* one. The spectra data for all of the compounds are collected in Table 1.

The electrochemical properties of the laddered APBDs and ligands were studied by cyclic voltammetry. All of the compounds displayed reversible redox waves in CH_2Cl_2 (see the Supporting Information). The coordination of the BF_2 groups slightly changes the oxidation potential but increases the reduction potential obviously for the laddered APBDs. The energies of the HOMOs and LUMOs, together with the HOMO−LUMO energy gaps, were estimated from the redox potentials, as shown in Table 1. The subtle differences of the oxidation potentials among the laddered compounds indicate that the incorporation of boron has a negligible influence on the HOMO energy. Thus, the gradual decrease in the HOMO−LUMO gap upon boron chelation can be attributed to the enhanced conjugation, which decreases the LUMO energy significantly. The HOMO−LUMO gaps estimated from absorption spectra onset are consistent with the electrochemical results (Table 1).

To obtain a better understanding of the photophysical and electronic properties of the ladder-type APBDs, theoretical calculations were performed using the Gaussian 09 suite of programs. The HOMO and LUMO diagrams are shown in Figure 3. It is noteworthy that the electron density of the HOMO is predominantly distributed along the carbazole unit, exhibiting the character of a carbazole π system, while the electron density of the LUMO is considerably delocalized over the pyrimidine or pyrazine group. Thus, the locations of the HOMO and LUMO depict a perpendicular arrangement that outlines the ladder structure of the APBDs. The theoretical values determined for the frontier orbital energies are in approximate agreement with the experimental data (Table 1). The energy gap follows the trend **8** (1.58 eV) < **5** (2.07 eV) < **7** (2.41 eV) < **4** (2.73 eV) < **6** (3.22 eV) < **3** (3.93 eV). The *anti*-laddered APBDs exhibit lower HOMO−LUMO energy gaps

Table 1. Spectral and Electrochemical Data of the Ligands and Ladder-Type APBDs[a]

	3	4	5	6	7	8
λ_{abs} (nm)	410	493	586	424	500	620
$10^{-4}\varepsilon$ (M^{-1} cm^{-1})	3.48	5.50	4.27	5.44	2.97	0.76
λ_{em} (nm)	no	567	645	no	no	no
Φ_f	no	0.18	0.06	no	no	no
E_{ox} (V)	0.99	1.02	1.09	0.90	0.92	1.06
E_{red} (V)	−1.16	−1.13	−0.92	−1.17	−0.98	−0.64
E_{LUMO}[b] (eV)	−3.44 [−1.54]	−3.47 [−2.75]	−3.68 [−3.65]	−3.43 [−1.85]	−3.62 [−3.00]	−3.96 [−4.11]
E_{HOMO} (eV)[b]	−5.59 [−5.47]	−5.62 [−5.48]	−5.69 [−5.72]	−5.50 [−5.08]	−5.52 [−5.41]	−5.66 [−5.70]
E_{gap} (eV)[c]	2.15 (2.76) [3.93]	2.15 (2.25) [2.73]	2.01 (1.90) [2.07]	2.07 (2.67) [3.22]	1.90 (2.13) [2.41]	1.70 (1.59) [1.58]

[a]The values in square brackets are theoretical results. [b]Calculated from the empirical following formulas: $E_{LUMO} = -(E_{red} - E_{Fc/Fc^+} + 4.80\ eV)$; $E_{HOMO} = -(E_{ox} - E_{Fc/Fc^+} + 4.80\ eV)$. The measured value of E_{Fc/Fc^+} is 0.20 V vs Ag/Ag^+. [c]$E_{gap} = E_{LUMO} - E_{HOMO}$. The values in parentheses were estimated from absorption spectra onsets.

dx.doi.org/10.1021/jo402583y | J. Org. Chem. 2014, 79, 459−464

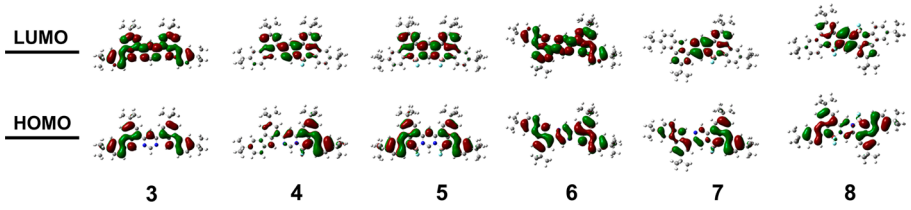

Figure 3. Frontier molecular orbital diagrams for **3**–**8** calculated using DFT.

than the corresponding *syn* ones, suggesting enhanced conjugation in the *anti* series. This is consistent with the trend observed by the UV–vis absorption spectroscopy. Time-dependent DFT calculations were also performed to understand the absorption properties. The contribution of the molecular orbitals involved in the UV–vis transitions was determined on the basis of their oscillator strengths (*f*). According to the calculated results, the lower-energy bands in the absorption spectra show a preferential correspondence with the HOMO → LUMO and HOMO−1 → LUMO transitions. Overall, the theoretical calculations fully support the electrochemical and photophysical properties of these novel laddered APBDs.

In summary, we have accomplished the synthesis of a series of *syn*- and *anti*-ladder-type APBDs by a Suzuki–Miyaura coupling reaction and stepwise incorporation with boron. The single-crystal X-ray diffraction analysis of **3** unambiguously confirmed the formation of the ladder structure. The UV/vis absorption and fluorescence spectra indicate that there exists effective π-delocalization in the ladder-type APBDs. The electrochemical experiments as well as the theoretical calculations revealed that the energy of the lowest unoccupied molecular orbital is substantially decreased upon boron chelation, which is essential for the performance of organic electronic devices with high electron affinities and mobilities, reinforcing a potential application of the APBDs in the area of organic electronics.

EXPERIMENTAL SECTION

General Information. Reagents were used without further purification, unless otherwise noted. 1, 4-Dioxane, toluene, and DMF were dried with sodium or CaH_2 and distilled under a N_2 atmosphere. ^{1}H NMR (400 MHz), ^{13}C NMR (100 MHz), and ^{19}F NMR (376 MHz) spectra were obtained from a spectrometer with tetramethylsilane as an internal standard. Mass spectra were measured by MALDI-TOF or high-resolution ESI-TOF experiments. Absorption and emission spectra were recorded in a conventional quartz cell (10 mm light path) on a standard, commercial spectrometer. Fluorescence quantum yields were determined with excitation at 500 nm using zinc tetraphenylporphyrin (Zn-TPP) as a standard. X-ray data were taken on a diffractometer with Mo Kα radiation (λ = 0.71073 Å). The redox potentials of the compounds were determined by cyclic voltammetry using glassy carbon as the working electrode, platinum as the counter electrode, and nonaqueous Ag/Ag^+ as the reference electrode in the presence of 0.1 M Bu_4NPF_6 as the supporting electrolyte. The working electrode was polished with a 0.05 μm alumina paste and washed with water and acetone by sonication before use. The electrolyte solution was purged with argon for 20 min before measurement.

1-Bromo-3,6-di-*tert*-butyl-9*H*-carbazole (1). Compound **1** was synthesized according to the reported procedure.[48] ^{1}H NMR (400 MHz, $CDCl_3$): δ 8.06 (d, J = 1.6 Hz, 1H), 8.05 (s, 1H), 8.03 (d, J = 1.4 Hz, 1H), 7.61 (d, J = 1.5 Hz, 1H), 7.52 (dd, J = 8.6, 1.8 Hz, 1H), 7.40 (d, J = 8.5 Hz, 1H), 1.47 (d, J = 3.6 Hz, 18H).

1-Boryl-3,6-di-*tert*-butyl-9*H*-carbazole (2). Compound **1** (358.0 mg, 1.0 mmol, 1.0 equiv) and $Pd(PPh_3)_2Cl_2$ (70.2 mg, 0.1 mmol, 0.1 equiv) were added to a Schlenk flask, which was purged with argon and then charged with pinacolborane (0.8 mL, 5.0 mmol, 5.0 equiv), Et_3N (1.49 mL), and 1,4-dioxane (4 mL). The mixture was stirred at reflux for 3 h under argon. After removal of solvents under vacuum, the crude product was purified by column chromatography on silica gel (CH_2Cl_2/petroleum ether = 1/4) and recrystallized from a mixture of dichloromethane and petroleum ether to afford **2** (345 mg, 85%) as a white solid. ^{1}H NMR (400 MHz, $CDCl_3$): δ 8.96 (s, 1H), 8.22 (d, J = 2.0 Hz, 1H), 8.08 (d, J = 1.6 Hz, 1H), 7.89 (d, J = 2.0 Hz, 1H), 7.47 (dd, J = 8.5, 1.9 Hz, 1H), 7.40 (d, J = 8.5 Hz, 1H), 1.50–1.41 (m, 30H).

General Procedure for the Ligand Synthesis by Suzuki–Miyaura Coupling Reaction. Compound **2** (3.0 equiv), the dichloro- or dibromo-substituted bridge (1.0 equiv), $Pd(PPh_3)_4$ (0.1 equiv), Cs_2CO_3 (2.0 equiv), and CsF (2.0 equiv) were added to a Schlenk flask, which was purged with argon and then charged with dried toluene and DMF (2/1 v/v). The resulting mixture was degassed thoroughly through three freeze–pump–thaw cycles and then stirred at 90 °C for 12 h under argon. The reaction was quenched with water, and the mixture was extracted with CH_2Cl_2. The organic layer was dried over anhydrous sodium sulfate. After removal of the solvent under vacuum, the residue was purified by column chromatography on silica gel to afford the desired product.

*syn-Laddered Ligand **3**.* Ligand **3** was prepared by the Suzuki–Miyaura coupling reaction of **2** (121.6 mg, 0.3 mmol, 3.0 equiv) with 4,6-dichloropyrimidine (14.9 mg, 0.1 mmol, 1.0 equiv) according to the general procedure and purified by column chromatography on silica gel (CH_2Cl_2/petroleum ether = 1/2) and recrystallization from *n*-hexane/CH_2Cl_2 (1/4) to afford **3** as a yellow solid (44.4 mg, 70% yield). ^{1}H NMR (400 MHz, $CDCl_3$): δ 11.06 (s, 2H), 9.51 (s, 1H), 8.60 (s, 1H), 8.33 (d, J = 1.3 Hz, 2H), 8.21 (d, J = 1.4 Hz, 2H), 8.16 (s, 2H), 7.60–7.52 (m, 4H), 1.58 (s, 18H), 1.49 (s, 19H). ^{13}C NMR (100 MHz, $CDCl_3$): δ 164.9, 158.0, 142.7, 141.9, 138.6, 138.0, 125.7, 124.5, 122.5, 121.1, 120.6, 117.3, 116.5, 111.1, 110.9, 35.1, 32.3. MS (MALDI-TOF) m/z: calcd for $C_{44}H_{50}N_4$, 634.4 $[M]^+$; found, 634.4. HR-MS (ESI-TOF) m/z: calcd for $C_{44}H_{50}N_4Na$, 657.3933 $[M + Na]^+$; found, 657.3929 $[M + Na]^+$.

*anti-Laddered Ligand **6**.* Ligand **6** was prepared by the Suzuki–Miyaura coupling reaction of **2** (121.6 mg, 0.3 mmol, 3.0 equiv) with 2,5-dibromopyrazine (23.8 mg, 0.1 mmol, 1.0 equiv) according to the general procedure and purified by column chromatography on silica gel (CH_2Cl_2/petroleum ether = 1/2) and recrystallization from *n*-hexane/CH_2Cl_2 (1/4) to afford **6** as a yellow solid (60.3 mg, 95% yield). ^{1}H NMR (400 MHz, $CDCl_3$): δ 10.87 (s, 2H), 9.55 (s, 2H), 8.26 (s, 2H), 8.17 (d, J = 17.3 Hz, 4H), 7.61–7.42 (m, 4H), 1.60 (m, 36H). ^{13}C NMR (100 MHz, $CDCl_3$): δ 150.1, 142.6, 142.1, 140.1, 138.5, 137.7, 125.4, 124.4, 122.8, 120.2, 119.0, 117.0, 116.5, 110.8, 35.1, 32.3. MS (MALDI-TOF) m/z: calcd for $C_{44}H_{50}N_4$, 634.4 $[M]^+$; found, 634.4. HR-MS (ESI-TOF) m/z: calcd for $C_{44}H_{50}N_4Na$, 657.3933 $[M + Na]^+$; found, 657.3925 $[M + Na]^+$.

General Procedure for the Synthesis of Ladder-Type APBDs. The laddered ligand (**3** or **6**) (1.0 equiv) and toluene were added to a three-neck flask, and then triethylamine (3.0 or 10.0 equiv) was added to the reaction mixture. After the mixture was stirred at room temperature for 15 min, $BF_3{\cdot}OEt_2$ (3.0 or 10.0 equiv) was added dropwise. The reaction mixture was stirred at 80 °C for 1 or 3 h under argon and then cooled to room temperature. The reaction was quenched with water, and the mixture was extracted with CH_2Cl_2. The organic layer was washed with water and dried over anhydrous sodium sulfate. After removal of the solvent under vacuum, the residue was

dx.doi.org/10.1021/jo402583y | J. Org. Chem. 2014, 79, 459–464

purified by column chromatography on silica gel to afford the desired product.

syn-Ladder-Type APBD **4**. APBD **4** was prepared by the reaction of **3** (63.5 mg, 0.1 mmol, 1.0 equiv), triethylamine (43 μL, 0.3 mmol, 3.0 equiv), and $BF_3{\cdot}OEt_2$ (38 μL, 0.3 mmol, 3.0 equiv), upon stirring at 80 °C for 1 h according to the general procedure and purified by column chromatography on silica gel (CH_2Cl_2/petroleum ether = 1/3) and recrystallized from *n*-hexane/CH_2Cl_2 (1/4) to afford ladder-type APBD **4** as an orange solid (44.4 mg, 65% yield). ^{1}H NMR (400 MHz, $CDCl_3$): δ 10.73 (s, 1H), 9.57 (s, 1H), 8.62 (s, 1H), 8.34 (d, *J* = 11.7 Hz, 2H), 8.12 (s, 3H), 7.89 (s, 1H), 7.80 (d, *J* = 8.4 Hz, 1H), 7.62−7.49 (m, 3H), 1.65−1.40 (m, 36H). ^{13}C NMR (100 MHz, $CDCl_3$): δ 166.0, 153.4, 138.4, 125.4, 125.2, 123.4, 121.9, 118.1, 116.7, 113.4, 111.0, 108.0, 35.2, 35.0, 32.5. ^{19}F NMR (376 MHz, $CDCl_3$): δ −133.1. MS (MALDI-TOF) *m*/*z*: calcd for $C_{44}H_{49}BF_2N_4$, 682.4 $[M]^+$; found, 682.5 $[M]^+$. HR-MS (ESI-TOF) *m*/*z*: calcd for $C_{44}H_{50}N_4Na$, 657.3933 $[M - BF_2 + Na]^+$; found, 657.3948.

syn-Ladder-Type APBD **5**. APBD **5** was prepared by the reaction of **3** (63.5 mg, 0.1 mmol, 1.0 equiv), triethylamine (139 μL, 1.0 mmol, 10.0 equiv), and $BF_3{\cdot}OEt_2$ (124 μL, 1.0 mmol, 10.0 equiv) upon stirring at 80 °C for 3 h according to the general procedure and purified by column chromatography on silica gel (CH_2Cl_2/petroleum ether = 1/3) and recrystallized from *n*-hexane/CH_2Cl_2 (1/4) to afford ladder-type APBD **5** as a purple-black solid (58.4 mg, yield 80%). ^{1}H NMR (400 MHz, $CDCl_3$): δ 9.87 (s, 1H), 8.62 (s, 1H), 8.52 (s, 2H), 8.13 (s, 2H), 8.09 (s, 2H), 7.84 (d, *J* = 8.4 Hz, 2H), 7.66 (d, *J* = 9.2 Hz, 2H), 1.59 (s, 19H), 1.48 (s, 18H). ^{13}C NMR for **5** was unreadable because of low solubility. ^{19}F NMR (376 MHz, $CDCl_3$): δ −131.6. MS (MALDI-TOF) *m*/*z*: calcd for $C_{44}H_{48}B_2F_4N_4$, 730.4 $[M]^+$; found, 730.5 $[M]^+$. HR-MS (ESI-TOF) *m*/*z*: calcd for $C_{44}H_{50}N_4Na$, 657.3933 $[M - 2(BF_2) + Na]^+$; found, 657.3908.

anti-Ladder-Type APBD **7**. APBD **7** was prepared by the reaction of **6** (63.5 mg, 0.1 mmol, 1.0 equiv), triethylamine (43 μL, 0.3 mmol, 3.0 equiv), and $BF_3{\cdot}OEt_2$ (38 μL, 0.3 mmol, 3.0 equiv) upon stirring at 80 °C for 1 h according to the general procedure and purified by column chromatography on silica gel (CH_2Cl_2/petroleum ether = 1/3) and recrystallized from *n*-hexane/CH_2Cl_2 (1/4) to afford ladder-type APBD **7** as a red solid (46.4 mg, yield 68%). ^{1}H NMR (400 MHz, $CDCl_3$): δ 10.61 (s, 1H), 10.00 (s, 1H), 9.42 (s, 1H), 8.40 (s, 1H), 8.33 (s, 1H), 8.22 (s, 1H), 8.16 (s, 2H), 8.10 (s, 1H), 7.86 (d, *J* = 8.4 Hz, 1H), 7.65 (d, *J* = 8.6 Hz, 1H), 7.58 (d, *J* = 8.4 Hz, 1H), 7.50 (d, *J* = 8.5 Hz, 1H), 1.53 (s, 36H). ^{13}C NMR (100 MHz, $CDCl_3$): δ 152.4, 144.1, 143.3, 142.8, 138.4, 137.1, 131.2, 125.9, 125.3, 124.8, 124.4, 123.5, 122.5, 120.8, 120.2, 117.5, 117.0, 116.6, 115.2, 113.5, 110.9, 108.5, 47.3, 35.4, 35.3, 32.3. ^{19}F NMR (376 MHz, $CDCl_3$): δ −133.1. MS (MALDI-TOF) *m*/*z*: calcd for $C_{44}H_{49}BF_2N_4$, 682.4 $[M]^+$; found, 682.4. HR-MS (ESI-TOF) *m*/*z*: calcd for $C_{44}H_{50}N_4Na$, 657.3933 $[M - BF_2 + Na]^+$; found, 657.3981.

anti-Ladder-Type APBD **8**. APBD **8** was prepared by the reaction of **3** (63.5 mg, 0.1 mmol, 1.0 equiv), triethylamine (139 μL, 1.0 mmol, 10.0 equiv), and $BF_3{\cdot}OEt_2$ (124 μL, 1.0 mmol, 10.0 equiv) with stirring at 80 °C for 3 h according to the general procedure and purified by column chromatography on silica gel (CH_2Cl_2/petroleum ether = 1/3) and recrystallized from *n*-hexane/CH_2Cl_2 to afford *anti*-ladder-type APBD **8** as a purple-black solid (62.1 mg, yield 85%). ^{1}H NMR (400 MHz, $CDCl_3$): δ 9.80 (s, 2H), 8.47 (s, 2H), 8.16 (s, 2H), 8.09 (s, 2H), 7.84 (d, *J* = 8.6 Hz, 2H), 7.67 (d, *J* = 8.5 Hz, 2H), 1.60−1.47 (m, 36H). ^{13}C NMR for **8** was unreadable because of low solubility. ^{19}F NMR (376 MHz, $CDCl_3$): δ −129.9. MS (MALDI-TOF) *m*/*z*: calcd for $C_{44}H_{48}B_2F_4N_4$, 730.4 $[M]^+$; found, 730.5. HR-MS (ESI-TOF) *m*/*z*: calcd for $C_{44}H_{50}N_4K$, 673.3673 $[M - 2(BF_2) + K]^+$; found, 673.3607.

■ ASSOCIATED CONTENT

Ⓢ Supporting Information

NMR and MS spectra, fluorescence spectra, cyclic voltammetry, atom coordinates and absolute energies from DFT calculations, and the CIF file and crystal data for **3**. This material is available free of charge via the Internet at http://pubs.acs.org. The crystallographic data for **3** have been deposited with the Cambridge Crystallographic Data Centre as CCDC 952228.

■ AUTHOR INFORMATION

Corresponding Authors

*E-mail: yili@mail.ipc.ac.cn.
*E-mail: chenjp@mail.ipc.ac.cn.
*E-mail: gqyang@iccas.ac.cn.

Notes

The authors declare no competing financial interest.

■ ACKNOWLEDGMENTS

Financial support by the National Natural Science Foundation of China (Grants 21172229 and 21233011) and the National Basic Research Program of China (Grants 2013CB834700, 2010CB934500, and 2013CB834505) is gratefully acknowledged. J.C. thanks the Beijing Nova Program for financial support.

■ REFERENCES

(1) Roncali, J. *Acc. Chem. Res.* **2009**, *42*, 1719.
(2) Mishra, A.; Bauerle, P. *Angew. Chem., Int. Ed.* **2012**, *51*, 2020.
(3) Ameri, T.; Khoram, P.; Min, J.; Brabec, C. J. *Adv. Mater.* **2013**, *25*, 4245.
(4) Kulkarni, A. P.; Tonzola, C. J.; Babel, A.; Jenekhe, S. A. *Chem. Mater.* **2004**, *16*, 4556.
(5) Wong, K.-T.; Liao, Y.-L.; Lin, Y.-T.; Su, H.-C.; Wu, C.-c. *Org. Lett.* **2005**, *7*, 5131.
(6) Burn, P. L.; Lo, S. C.; Samuel, I. D. W. *Adv. Mater.* **2007**, *19*, 1675.
(7) Shirota, Y.; Kageyama, H. *Chem. Rev.* **2007**, *107*, 953.
(8) Wang, C.; Dong, H.; Hu, W.; Liu, Y.; Zhu, D. *Chem. Rev.* **2012**, *112*, 2208.
(9) Mei, J.; Diao, Y.; Appleton, A. L.; Fang, L.; Bao, Z. *J. Am. Chem. Soc.* **2013**, *135*, 6724.
(10) Murphy, A. R.; Fréchet, J. M. J. *Chem. Rev.* **2007**, *107*, 1066.
(11) Jacob, J.; Sax, S.; Piok, T.; List, E. J. W.; Grimsdale, A. C.; Müllen, K. *J. Am. Chem. Soc.* **2004**, *126*, 6987.
(12) Kawaguchi, K.; Nakano, K.; Nozaki, K. *J. Org. Chem.* **2007**, *72*, 5119.
(13) Hertel, D.; Scherf, U.; Bassler, H. *Adv. Mater.* **1998**, *10*, 1119.
(14) Balandier, J.-Y.; Henry, N.; Arlin, J.-B.; Sanguinet, L.; Lemaur, V.; Niebel, C.; Chattopadhyay, B.; Kennedy, A. R.; Leriche, P.; Blanchard, P.; Cornil, J.; Geerts, Y. H. *Org. Lett.* **2013**, *15*, 302.
(15) Zhu, X.; Tsuji, H.; López Navarrete, J. T.; Casado, J.; Nakamura, E. *J. Am. Chem. Soc.* **2012**, *134*, 19254.
(16) Laquai, F.; Mishra, A. K.; Ribas, M. R.; Petrozza, A.; Jacob, J.; Akcelrud, L.; Müllen, K.; Friend, R. H.; Wegner, G. *Adv. Funct. Mater.* **2007**, *17*, 3231.
(17) Ahmed, E.; Earmme, T.; Ren, G.; Jenekhe, S. A. *Chem. Mater.* **2010**, *22*, 5786.
(18) Iida, A.; Saito, S.; Sasamori, T.; Yamaguchi, S. *Angew. Chem., Int. Ed.* **2013**, *52*, 3760.
(19) Zhou, Z. G.; Wakamiya, A.; Kushida, T.; Yamaguchi, S. *J. Am. Chem. Soc.* **2012**, *134*, 4529.
(20) Saito, S.; Matsuo, K.; Yamaguchi, S. *J. Am. Chem. Soc.* **2012**, *134*, 9130.
(21) Elbing, M.; Bazan, G. C. *Angew. Chem., Int. Ed.* **2008**, *47*, 834.
(22) Wakamiya, A.; Mori, K.; Yamaguchi, S. *Angew. Chem., Int. Ed.* **2007**, *46*, 4273.
(23) Jäkle, F. *Chem. Rev.* **2010**, *110*, 3985.
(24) Araneda, J. F.; Neue, B.; Piers, W. E. *Angew. Chem., Int. Ed.* **2012**, *51*, 9977.
(25) Li, D.; Yuan, Y.; Bi, H.; Yao, D.; Zhao, X.; Tian, W.; Wang, Y.; Zhang, H. *Inorg. Chem.* **2011**, *50*, 4825.
(26) Fukazawa, A.; Yamaguchi, E.; Ito, E.; Yamada, H.; Wang, J.; Irle, S.; Yamaguchi, S. *Organometallics* **2011**, *30*, 3870.

(27) Araneda, J. F.; Neue, B.; Piers, W. E.; Parvez, M. *Angew. Chem., Int. Ed.* **2012**, *51*, 8546.
(28) Mercier, L. G.; Piers, W. E.; Harrington, R. W.; Clegg, W. *Organometallics* **2013**, *32*, 6820.
(29) Curiel, D.; Más-Montoya, M.; Usea, L.; Espinosa, A.; Orenes, R. A.; Molina, P. *Org. Lett.* **2012**, *14*, 3360.
(30) Meltola, N. J.; Wahlroos, R.; Soini, A. E. *J. Fluoresc.* **2004**, *14*, 635.
(31) Niu, S. L.; Massif, C.; Ulrich, G.; Ziessel, R.; Renard, P. Y.; Romieu, A. *Org. Biomol. Chem.* **2011**, *9*, 66.
(32) Niu, S. L.; Massif, C.; Ulrich, G.; Renard, P. Y.; Romieu, A.; Ziessel, R. *Chem.—Eur. J.* **2012**, *18*, 7229.
(33) Golovkova, T. A.; Kozlov, D. V.; Neckers, D. C. *J. Org. Chem.* **2005**, *70*, 5545.
(34) Rurack, K.; Kollmannsberger, M.; Daub, J. *Angew. Chem., Int. Ed.* **2001**, *40*, 385.
(35) Trieflinger, C.; Rurack, K.; Daub, J. *Angew. Chem., Int. Ed.* **2005**, *44*, 2288.
(36) Boens, N.; Leen, V.; Dehaen, W. *Chem. Soc. Rev.* **2012**, *41*, 1130.
(37) Niu, L.-Y.; Guan, Y.-S.; Chen, Y.-Z.; Wu, L.-Z.; Tung, C.-H.; Yang, Q.-Z. *J. Am. Chem. Soc.* **2012**, *134*, 18928.
(38) Niu, L.-Y.; Guan, Y.-S.; Chen, Y.-Z.; Wu, L.-Z.; Tung, C.-H.; Yang, Q.-Z. *Chem. Commun.* **2013**, *49*, 1294.
(39) Ziessel, R.; Harriman, A. *Chem. Commun.* **2011**, *47*, 611.
(40) Yilmaz, M. D.; Bozdemir, O. A.; Akkaya, E. U. *Org. Lett.* **2006**, *8*, 2871.
(41) Bozdemir, O. A.; Yilmaz, M. D.; Buyukcakir, O.; Siemiarczuk, A.; Tutas, M.; Akkaya, E. U. *New J. Chem.* **2010**, *34*, 151.
(42) Yen, Y.-S.; Chou, H.-H.; Chen, Y.-C.; Hsu, C.-Y.; Lin, J. T. *J. Mater. Chem.* **2012**, *22*, 8734.
(43) Erten-Ela, S.; Yilmaz, M. D.; Icli, B.; Dede, Y.; Icli, S.; Akkaya, E. U. *Org. Lett.* **2008**, *10*, 3299.
(44) Kumaresan, D.; Thummel, R. P.; Bura, T.; Ulrich, G.; Ziessel, R. *Chem.—Eur. J.* **2009**, *15*, 6335.
(45) Loudet, A.; Burgess, K. *Chem. Rev.* **2007**, *107*, 4891.
(46) Ulrich, G.; Ziessel, R.; Harriman, A. *Angew. Chem., Int. Ed.* **2008**, *47*, 1184.
(47) Araneda, J. F.; Piers, W. E.; Heyne, B.; Parvez, M.; McDonald, R. *Angew. Chem., Int. Ed.* **2011**, *50*, 12214.
(48) Gibson, V. C.; Spitzmesser, S. K.; White, A. J. P.; Williams, D. J. *Dalton Trans.* **2003**, 2718.

dx.doi.org/10.1021/jo402583y | *J. Org. Chem.* 2014, 79, 459−464